

Simulation model for shot peening indent topography on case carburized gear steel

Erland Nordin^{a,b}, Bo Alfredsson^b

^a Scania CV AB, Sweden, erlandn@kth.se, ^b Solid Mechanics at Royal Institute of Technology KTH, Sweden

Keywords: dynamic indentation, shot peening, strain rate dependence, retained austenite transformation

Abstract

Simulation of shot peening on case carburized gear steel demands a material model that include strain rate dependence and martensite transformation. Determining the material parameters is a challenging task due to the mechanical and fracture behaviour of hardened gear steel. A material model and its influence on indent topography during dynamic indentation is presented that will allow reverse modelling of the model parameters using experimental confocal measurements of indent profiles at different velocities.

Introduction

Case carburized gear steels typically contain around 20 – 30 % retained austenite. During shot peening the austenite transforms partially to martensite due to stress-assisted and strain-induced martensite transformation [1]. A simulation model appropriate for gear steels should thus include not only a strain rate dependent constitutive material model but also the effects of martensite transformation. A great challenge is however the determination of the numerous material parameters for such a model. The stress-assisted transformation can be measured in a well-equipped solid mechanics laboratory as presented by Neu and Sehitoglu [2] but strain-induced transformation is much more difficult because of the high hardness and brittleness of the case material in gears.

The strain rates during shot peening can reach $10^5 - 10^6$ 1/s which is not possible to measure with a Split-Hopkinson bar equipment. One alternative to determine strain rate parameters for shot peening was presented by Nordin *et al.* [3]. The method consists of impacting the target material with carbide balls at different velocities and measuring the indent profiles with a confocal microscope. The material parameters are then determined through reverse modelling by fitting all the impact profiles to simulations. A similar approach could be used to determine suitable parameters for the martensite transformation. This paper presents a study on the influence of some important material parameters on the indent profile. The influence on indent diameter, depth, pile-up and general profile shape is presented which can be used while reverse modelling indent profiles at different velocities.

Model

The material model use kinematic hardening with three back stresses for the work hardening behaviour, parameters $(C_1 - C_3, g_1 - g_3, \sigma_0)$. The yield stress is increased by the strain rate using the Johnson-Cook formulation, parameters $(C_{JC}, \dot{\epsilon}_0)$ [4]. Martensite fraction f_m is assumed to follow the Koistinen-Marburger equation where the martensitic start temperature M_s is offset by the stress (ΔM_s) , the plastic strain (ΔM_{pl}) state and M_{ss} which will be defined later.

$$f_m = 1 - e^{-k(M_s + \Delta M_s + \Delta M_{pl} + M_{ss} - T)} \quad (1)$$

The factor k is determined by the definition that the martensite content is 99% when the temperature T reaches M_f during quenching. Therefore

$$k = \frac{4.605}{M_s - M_f} \quad (2)$$

where M_f is the martensite finish temperature during quenching.

It is well known that a hydrostatic tensile stress will promote retained austenite transformation while hydrostatic compressive stress will reduce it [5]. A shear stress will also promote transformation and therefore the temperature adjustment is formulated as an equation of the hydrostatic stress and the von Mises equivalent stress. The shift in martensitic start temperature due to applied stress is used according to Denis *et al.* [6],

$$\Delta M_s = a_1 \sigma_m + a_2 \sigma_e \quad (3)$$

where σ_m is the mean stress and σ_e the effective von Mises stress. The factors a_1 and a_2 in equation (3) is used to set the influence of each stress state. For an easier interpretation the ratio of mean stress over von Mises stress influence is introduced as $r_{ME} = a_1/a_2$.

The strain-induced effect on the martensite transformation has a sigmoidal shape which is modelled by Olson and Cohen [7] as,

$$\Delta M_{pl} = p_f (1 - e^{-\alpha \varepsilon_{pl}})^n = p_f (f^{sb})^n \quad (4)$$

where ε_{pl} is the plastic strain, f^{sb} is the shear band fraction, n determine the shape of the sigmoidal curve, α how fast it saturates and p_f the maximum value. Considerable work has been done by different researchers to extend this model by including e.g. temperature and stress state dependence or to give it a more physical foundation. The majority of the work done has however been on austenitic stainless steel [8]. The parameter ranges found and the more detailed models are therefore not necessarily applicable to case hardened and tempered steel with retained austenite. To facilitate easier fitting of this model to impact experiments, the simple model by Olson and Cohen in equation (4) is therefore preferred in this work. Because this steel has 65 % martensite the shear band equation cannot start from zero as it does for austenitic steels. As a reasonable approximation the fraction of shear bands is set equal to the fraction of initial martensite. The increase in shear band fraction (Δf^{sb}) is calculated with the rate form

$$\Delta f^{sb} = (1 - f^{sb}) \alpha \Delta \varepsilon_{pl} \quad (5)$$

Tempering the steel after quenching will stabilize the retained austenite and there will therefore be a limiting value of stress or temperature before the transformation can continue. This is included as a shift in temperature, M_{ss} , in the Koistinen-Marburger equation (1). To fulfil initial conditions the martensite shift is calculated as

$$M_{ss} = -\frac{1}{k} \ln(1 - f_{m,ini}) - M_s - p_f (f_{ini}^{sb})^n - \sigma_{lim} \left(a_2 + \frac{a_1}{3} \right) + T_{ini} \quad (6)$$

where $f_{m,ini}$ is the fraction of martensite initially, σ_{lim} is the uniaxial tensile stress for martensite transformation to start and T_{ini} is the experiment temperature. The volume expansion ΔV for the martensite transformation was chosen according to Moyer *et al.* [9] to $\Delta V = 0.037$. The deviatoric shape change followed the method applied by Serri *et al.* [10].

The model was fitted to the measurements by Neu and Sehitoglu [2] with the parameters shown in Table 1. The M_s and M_f temperatures were calculated with material properties simulation software JMatPro with 0.8 wt% carbon. Using common values for the alloy content of 4320 [11], the martensite start and end temperatures became $M_s = 169$ °C and $M_f = -101$ °C. The stress-strain response is compared to the experimental data by Neu and Sehitoglu [2] in Figure 1 (a) and the volumetric transformation strain in Figure 1 (b). The model fit the experimental data good except for the volumetric transformation strain in compression which however has a small and fluctuating value so that measurement seems uncertain.

With the initial conditions set in the Koistinen-Marburger expression in equation (1) the change in temperature to start transformation without any external stress field or plastic deformation can be calculated as

$$\Delta T = M_s + \Delta M_s + \Delta M_{pl} + M_{ss} \quad (7)$$

which gives $\Delta T = 63$ °C. With $T_{ini} = 22$ °C transformation starts at -41 °C. This is close to -45 °C reported by Neu and Sehitoglu [2] which shows that equations 1 - 6 are consistent with experimental observations.

Table 1: Model parameters used to fit the experimental data from Neu and Sehitoglu [2]. Consistent units with newton, second and millimeter has been used.

$f_{m,ini} = 0.65$	$T_{ini} = 22$ °C	$M_s = 169$ °C	$M_f = -101$ °C	$n = 4$
$C_1 = 15432$	$C_2 = 281622$	$C_3 = 470894$	$\sigma_0 = 769$	$\alpha = 4$
$g_1 = 5.0$	$g_2 = 236$	$g_3 = 2301$	$\Delta V = 0.037$	$p_f = 0$
$a_2 = 0.028$	$r_{ME} = 2.0$	$C_{JC} = 0.0$	$\dot{\epsilon}_0 = 1.0$	
$\sigma_{lim} = 485$	$E = 200 \cdot 10^3$	$\nu = 0.3$		

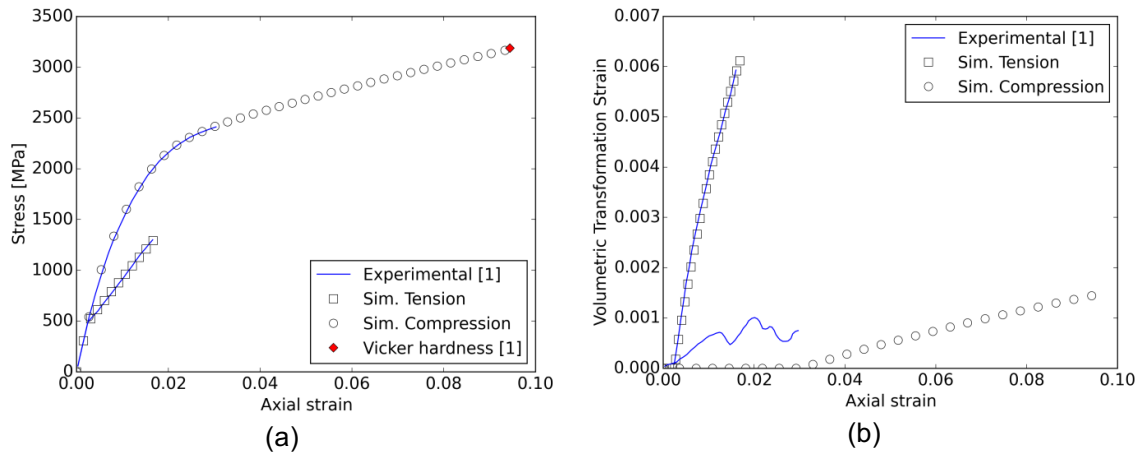


Figure 1: Comparison between experimental results by Neu and Sehitoglu [2] and model simulations with parameters in Table 1.

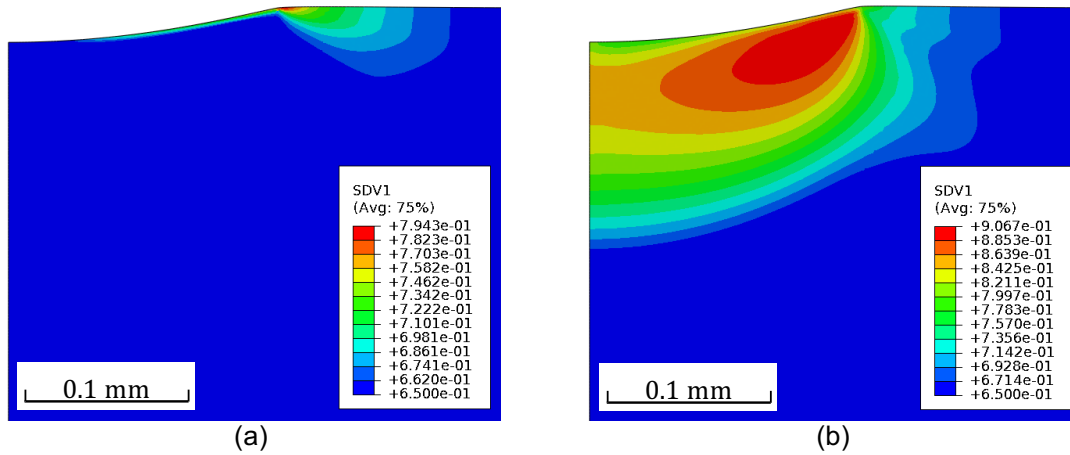


Figure 2: Fraction of martensite (SDV1) at an impact velocity of $V = 50$ m/s. Symmetry line of indent is along left edge. Stress-assisted transformation with parameters from Table 1 in (a) and combined stress and strain-induced transformation with $p_f = 400$ in (b).

Table 2: Indent diameter (d), depth (h) and pile-up for a case with no strain rate dependence or martensite transformation (noRA) compared in relative change in percent to different parameter variations.

$V = 20$ m/s	d [μm]	h [μm]	Pile-up [μm]		$V = 50$ m/s	d [μm]	h [μm]	Pile-up [μm]
noRA	213.54	7.87	0.38			327.88	20.61	1.14
	$\Delta \%$	$\Delta \%$	$\Delta \%$			$\Delta \%$	$\Delta \%$	$\Delta \%$
$r_{ME} = 2.0$	0.0	0.0	3.3			0.0	0.0	5.3
$r_{ME} = 1.0$	0.1	0.9	21.6			0.1	0.8	14.8
$r_{ME} = 0.5$	0.1	2.0	51.0			0.1	1.6	25.6
$r_{ME} = 0.0$	0.2	3.1	81.8			-1.0	2.4	37.5
$p_f = 100$	0.0	0.0	3.5			0.0	0.0	6.0
$p_f = 200$	0.0	0.0	3.8			0.0	-0.6	7.7
$p_f = 400$	0.0	-1.3	7.0			0.0	-1.0	41.1
$C_{JC} = 0.01$	-1.2	-2.5	0.4			-1.2	-1.7	2.6
$C_{JC} = 0.03$	-2.4	-8.6	-2.8			-2.5	-6.4	-0.5
$C_{JC} = 0.05$	-3.6	-14.3	-6.7			-3.7	-11.4	-1.5

$V = 80$ m/s	d [μm]	h [μm]	Pile-up [μm]		$V = 140$ m/s	d [μm]	h [μm]	Pile-up [μm]
noRA	406.72	33.29	1.97			522.62	58.37	3.66
	$\Delta \%$	$\Delta \%$	$\Delta \%$			$\Delta \%$	$\Delta \%$	$\Delta \%$
$r_{ME} = 2.0$	0.0	0.0	5.4			0.0	0.1	5.0
$r_{ME} = 1.0$	0.1	0.9	10.5			0.1	0.9	5.4
$r_{ME} = 0.5$	0.1	1.7	15.3			0.1	2.0	6.2
$r_{ME} = 0.0$	-1.0	2.6	21.5			-1.0	2.8	8.2
$p_f = 100$	0.0	-0.1	6.4			0.0	-0.3	7.6
$p_f = 200$	0.0	-0.5	13.5			0.0	0.0	23.4
$p_f = 400$	0.0	0.0	58.9			0.0	1.5	69.6
$C_{JC} = 0.01$	-0.1	-1.4	3.0			-0.1	-1.2	3.1
$C_{JC} = 0.03$	-1.4	-5.2	-0.5			-1.4	-4.1	-1.5
$C_{JC} = 0.05$	-2.6	-9.8	-2.2			-2.7	-8.1	-4.5

Result

The FEM-model used for the impact simulations is an axi-symmetric model explained in detail in Nordin and Alfredsson [12]. Figure 2 shows a contour plot of the martensite content in the indented target. In Figure 2 (a) the default model in Table 1 with only stress-assisted transformation has been used. The transformation only occurs at the edge of the contact where tensile stresses exist. Below the indenting sphere a large negative mean stress inhibits the transformation that would be induced if only the von Mises stress had been used for control of stress induced transformation. By lowering the r_{ME} ratio the influence of the mean stress decrease and martensite transformation would develop under the indent. Another option for transformation under the indent would be to activate the strain-induced parameter p_f . In Figure 2 (b) an example with $p_f = 400$ is shown, compare to $p_f = 0$ in (a). During the impact the high negative mean pressure inhibits the transformation below the indenting sphere just as in the previous case. However, when the ball rebound the mean pressure decrease and transformation starts due to the plastic strain contribution ΔM_{pl} . Transformation due to plastic deformation under the indent will therefore occur at the rebound of the ball. This decrease in retained austenite content is comparable to experimental results from shot peening on case carburized plates, Nordin and Alfredsson [1], suggesting that strain-induced transformation is the main contributor.

Table 2 shows the relative change in indent diameter, indent depth and pile-up when the parameters r_{ME} , p_f and C_{JC} were varied. There is only a small variation in indent diameter for strain rate dependence (C_{JC}). The indent depth is mostly influenced by the strain rate dependence and the relative change is the largest for the lowest impact velocities. The largest influence from the martensite transformation is seen on the pile-up. For the lower velocities the r_{ME} ratio influence most, but at higher velocities with larger plastic deformation the strain-induced parameter (p_f) dominate. Apart from the indent diameter, depth and pile-up, the profile shape also differ in ways that are difficult to quantify numerically. An example of that is shown in Figure 3. The strain-induced transformation create a sharp pile-up formation close to the indent edge while stress-assisted transformation with low mean stress dependence creates a pile-up far out from the indent.

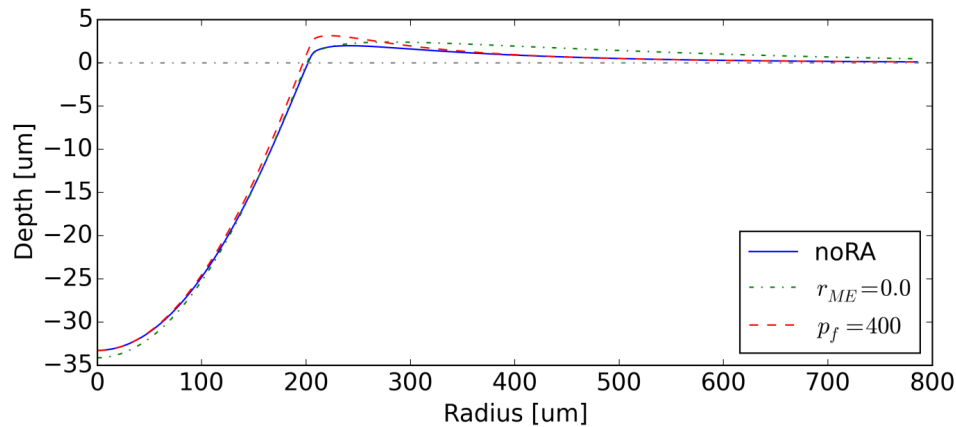


Figure 3: Profiles with no transformation (noRA), stress-assisted transformation with no mean stress dependence ($r_{ME} = 0$) and strain-induced transformation ($p_f = 400$).

Conclusions

The presented model makes it possible to simulate indentation and shot peening on case carburized gear steel. The model opens a method to determine material parameters which are required for accurate modelling and simulations of the complex material behaviour at shot peening. The mechanical and fracture behaviour of the material makes the parameters difficult to determine through other independent experiments. The strain rate has the largest influence on the indent diameter and depth while martensite transformation can affect the depth but mostly the pile-up dependence. Because the parameters affect the indent dimension and profile shape differently, both between each other and for different velocities, it will be possible to determine the model parameters from indent experiments similar to [3].

Acknowledgements

The authors would like to thank Scania CV AB for supporting this work.

References

- [1] Nordin E. and Alfredsson B., Experimental investigation of shot peening on case hardened SS2506 gear steel, *Experimental Techniques*, 2017
- [2] Neu R.W. and Sehitoglu H., Stress-induced transformation in a carburized steel - Experiments and analysis, *Acta Metallurgica Et Materialia*, vol 40, no: 9, pp 2257-2268, 1992
- [3] Nordin E., Ekström K., Alfredsson B., Experimental investigation of the strain rate dependence of SS2506 gear steel, *ICSP-12 Goslar Germany*, pp 564-569, 2014
- [4] Abaqus 6.14 Documentation, <https://www.3ds.com>, Visited 2017-04-21
- [5] Stringfellow R.G., Parks D.M., Olson G.B., A constitutive model for transformation plasticity accompanying strain-induced martensitic transformations in metastable austenitic steels, vol 40, no: 7, pp 1703-1716, 1992
- [6] Denis S., Gautier E., Simon A., Beck G., Stress-phase transformation interactions – basic principles, modelling, and calculation of internal stresses, *Materials Science and Technology*, vol 1, no: 10, pp 805-814, 1984
- [7] Olson G.B., Cohen M., Kinetics of strain-induced martensitic nucleation, *Metallurgical Transactions A*, vol 6, no: 4, pp 791-795, 1975
- [8] Tomita Y. and Iwamoto T., Constitutive modeling of trip steel and its application to the improvement of mechanical properties, *Int. J. Mech. Sci.*, vol 37, no: 12, pp 1295-1305, 1995
- [9] Moyer J.M. and Ansell G.S., The volume expansion accompanying the martensite transformation in iron-carbon alloys, *Metallurgical Transactions A*, vol 6, no: 9, pp 1785-1791, 1975
- [10] Serri J., Martiny M., Ferron Gérard, Finite element analysis of the effects of martensitic phase transformation in TRIP steel sheet forming, *Int. J. Mechanical Sciences*, vol 47, pp 884-901, 2005
- [11] Sieber R., Bending Fatigue Performance of Carburized Gear Steels, *SAE Technical Paper Series No. 920533*, 1992
- [12] Nordin E. and Alfredsson B., An elastic-plastic model for single shot-peening impacts, *Tribology Letters*, vol 52, no: 1, 2013